Rapid Communications

Fast, thin jets from bubbles expanding and collapsing in extreme vicinity to a solid boundary: A numerical study

Christiane Lechner,[1,2,*] Werner Lauterborn,[1] Max Koch,[1] and Robert Mettin[1]

[1]*Drittes Physikalisches Institut, Universität Göttingen, Friedrich-Hund-Platz 1, 37077 Göttingen, Germany*

[2]*Institute of Fluid Mechanics and Heat Transfer, TU Wien, Getreidemarkt 9, 1060 Vienna, Austria*

(Received 3 August 2018; published 5 February 2019)

A bubble expanding and collapsing in water near a flat solid boundary is studied numerically. According to current knowledge, it develops a high-speed liquid jet towards the boundary of typically ∼100 m/s. However, the character of jet formation and the jet properties alter strongly when the bubble expands and collapses very close to a solid boundary. In this case, a much thinner and much faster jet of typically ∼1000 m/s is generated. The respective mechanism is demonstrated by solving the Navier-Stokes equations for a model of a laser-induced bubble. The results add substantially to the understanding of the erosion process caused by imploding cavitation bubbles near solid boundaries.

DOI: 10.1103/PhysRevFluids.4.021601

It has been well known for more than a century that collapsing cavitation bubbles can damage the hardest materials. But despite elaborate experimental and numerical studies, the respective erosion process of solid surfaces by nearby bubbles is not yet fully understood (for experiments, see, e.g., Refs. [1–5], and for simulations, see Refs. [6–9], and the recent numerical results in Refs. [10–14]). While it is clear that the material damage occurs in connection with the strong collapse of expanded bubbles adjacent to the solid, the definite mechanisms are still a subject of research. A commonly considered candidate for erosion is the liquid jet that develops by involution of the top of the bubble (far side from the boundary) and rushes through the bubble towards the solid boundary. Typical jet speeds reach the order of 100 m/s, and upon impact high pressures are generated. Additionally, high pressures and shock waves are generated by the subsequent final collapse of the bubble. However, calculated jet impact and shock pressures from the described scenario stay partly below material yield stresses and might not be the definite answer to the erosion problem [15]. Here, we show that a different jet mechanism occurs for bubbles collapsing very close to the solid boundary, and that the resulting jet speeds may be higher by an order of magnitude.

An example of jet formation, that so far is considered in the scientific community, is given in Fig. 1. The simulation is done for a model of a laser-induced bubble in water at constant ambient pressure. Thereby, a small bubble with a high internal pressure is inserted into the liquid, here at a normalized distance of $D^* = 0.3$ ($D^* = D/R_{\max}$, with D the distance of the bubble center from the solid surface at generation and $R_{\max}$ the maximum radius the bubble would acquire in a free liquid). The bubble expands from its initial state to some maximum volume and collapses with the formation of an axial jet towards the boundary. In this case, with $R_{\max} = 500\ \mu$m and a static ambient pressure of 1 bar, it reaches a maximum velocity of 38 m/s and is quite broad in relation to the bubble extension. The bubble, now of toroidal shape, collapses further with the emission of shock waves [13].

*Corresponding author: christiane.lechner@tuwien.ac.at

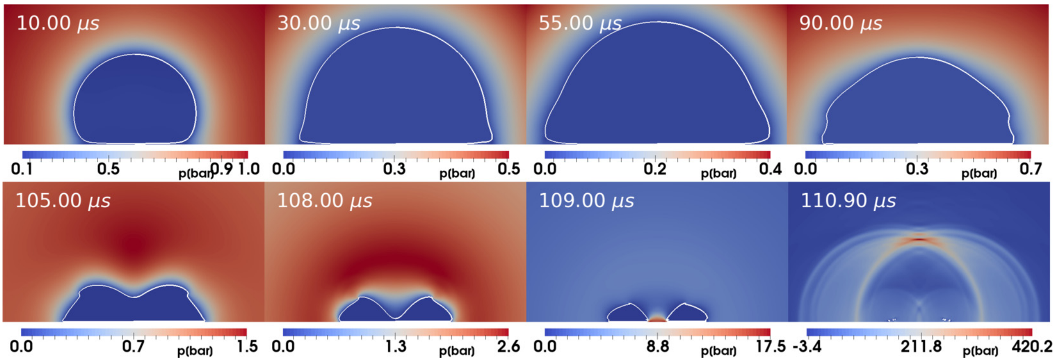

FIG. 1. Central cross section of bubble evolution under formation of a standard axial jet. The initial dimensionless distance of the bubble from the solid boundary is $D^* = 0.3$; $R_{\max} = 500\ \mu$m, static ambient pressure 1 bar. The wall is located at the lower border of each frame; frame size 1.4 mm × 0.75 mm (width × height). The color represents the pressure in bar (note the different scales in each frame). The bubble shape is indicated by the white lines. Simulations in axial symmetry with OpenFOAM.

However, in their seminal paper, Benjamin and Ellis [2] (Fig. 5 there) presented experimental results indicating that a bubble in very close vicinity ($D^* = 0.14$) to the wall develops a jet of different quality: a very thin and fast jet. Moreover, measurements of the jet velocity by Philipp and Lauterborn [4] showed that for a normalized distance of $D^* = 0.1$, the jet velocity is much larger than for $D^* = 0.3$, pointing to a jet of different quality for bubbles around $D^* = 0.1$, i.e., very near to a solid boundary. These experimental observations need to be supplemented with a theoretical explanation. This is done in the present Rapid Communication.

As a result, the view on jet formation has to be thoroughly changed for bubbles expanding and collapsing in very close proximity to a solid boundary. For the demonstration, a normalized distance of the bubble to the solid boundary of $D^* = 0.048$ is chosen. The bubble model is the standard one for a bubble in a cold liquid. The bubble contains a small amount of noncondensable gas (air) with adiabatic changes of state [12,16]. The liquid (water) is compressible according to the Tait equation [17]. Condensation and evaporation are neglected. Viscosity and surface tension are included. To simulate the dynamics of the bubble, the Navier-Stokes equations for a compressible Newtonian fluid are solved numerically with the help of the finite-volume package OpenFOAM [18]. The interface between the liquid and gas is captured with the volume of fluid method [19]. Simulations are performed in axial symmetry [20].

The shapes of the bubble with $D^* = 0.048$ upon expansion are given in the left diagram of Fig. 2 and upon collapse up to fast jet formation in the right diagram of Fig. 2. The bubble expands to an about hemispherical shape with a radius slightly larger than 600 μm with a quite sharp curvature at the outer rim near the solid boundary. Note in particular the liquid layer between the bubble and the wall that increases in height close to this outer rim. This is a consequence of the time-dependent viscous boundary layer that forms next to the solid wall during the expansion phase of the bubble. The resulting shape of the outer rim at maximum extension of the bubble is essential for the subsequent dynamics of the bubble and fast jet formation [21]. Upon collapse, the rim near the solid boundary soon starts to involute (Fig. 2, right diagram). The bubble develops a characteristic bell-shaped form (cf. Ref. [2], Fig. 5) with a spherical cap, an annular indentation, and a widening flank ($t = 105$ and 111 μs). The annular liquid flow towards the axis at the indentation gains a higher velocity than the downwards moving spherical cap. The situation is illustrated in Fig. 3 for $t = 111\ \mu$s and $t = 113.5\ \mu$s, where, in addition to the outline of the bubble, the velocity of the bubble wall is shown. Both the flow on top of the bubble and the annular flow gain speed during collapse. The annular flow approaches the axis of symmetry faster than the spherical cap advances.

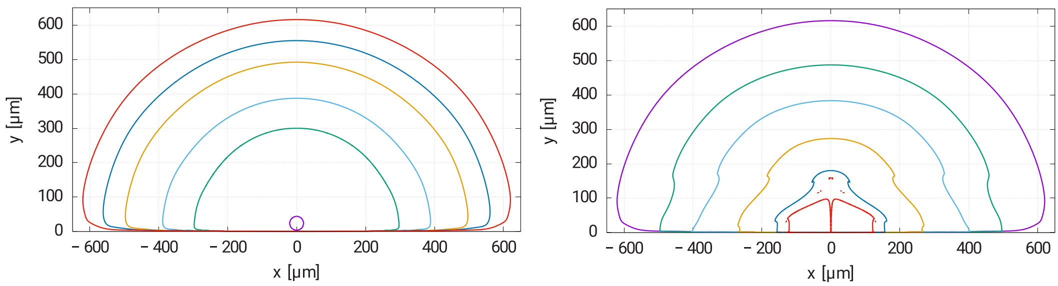

FIG. 2. Bubble shapes during expansion up to maximum volume (left diagram) and subsequent collapse (right diagram) for a bubble with $D^* = 0.048$. $R_{max} = 500$ μm, static ambient pressure 1 bar. The shapes are given at time instances $t = 0$, 5, 10, 20, 30, and 57 μs (left diagram, inner to outer curves), and $t = 57$, 95, 105, 111, 113.5, and 113.93 μs (right diagram, outer to inner curves).

It finally impacts at the axis with high velocity which leads to the formation of a thin, very fast axial jet through the bubble.

The very dynamics of the fast axial jet formation and subsequent dynamics for the bubble with $D^* = 0.048$ is presented in Fig. 4. The pressure field in the bubble region is shown in a series of plots from shortly before fast axial jet formation to shortly after the impact onto the opposite bubble wall that practically coincides with the solid boundary. The extremely thin, long, and fast axial jet is clearly seen in its formation, propagation, and impact. The annular liquid flow from the side impacts onto itself at the axis of symmetry just on top of the bubble or slightly below with pinch-off of a tiny bubble (113.84 μs). The second case has not been observed experimentally and only marginally affects the formation of the fast jet. The self-impact of the annular jet generates a high pressure at the impact site and accelerates the flow downwards into the bubble. Simultaneously, a strong shock wave is radiated from this point, whereas the bubble top involutes to form the fast jet (113.85 μs). The jet velocity shortly after formation (after 10 ns) amounts to $\gtrsim$2000 m/s. The jet is very thin, much thinner than the bubble diameter at this stage. It seems to be unstable and to decay into droplets upon propagation through the bubble. After the formation of the fast jet its propagation velocity stays about constant on its way through the bubble. The same holds for the slow jet at higher D^* [6,7,14]. Thus, the impact velocity onto the solid boundary stays at about 2000 m/s, considerably higher than the 38 m/s obtained for a bubble with $D^* = 0.3$. The impact pressure calculated for $D^* = 0.048$ is well above 20 000 bar, by far larger than the impact pressures at larger D^* [14].

Why does not the bubble of Fig. 1 with $D^* = 0.3$ develop a fast jet? This can be seen from the evolution of the bubble shape in the left diagram of Fig. 5. Here, again, an annular liquid inflow is

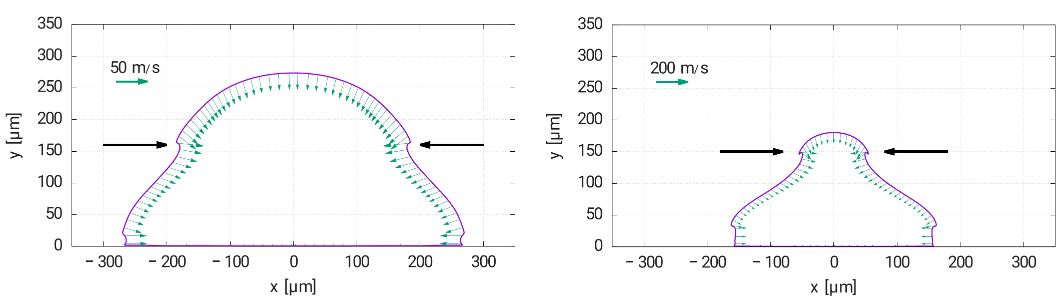

FIG. 3. Enlarged view of the bubble shapes at $t = 111$ μs (left diagram) and 113.5 μs (right diagram), together with the velocity of the bubble wall for the bubble in Fig. 2 ($D^* = 0.048$). The black arrows mark the location of the annular liquid inflow towards the axis that eventually outruns the collapse of the spherical cap.

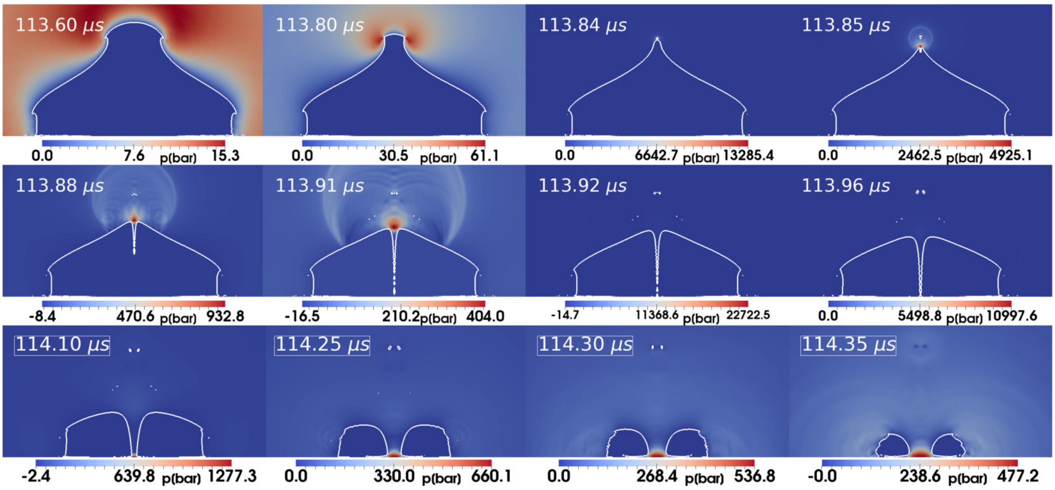

FIG. 4. Formation of the fast axial jet for a bubble with $D^* = 0.048$; $R_{\max} = 500\ \mu$m, static ambient pressure 1 bar; frame size 0.4 mm × 0.2 mm (width × height). The color indicates the pressure in bar (note the different scales in each frame). Impact of the liquid onto the axis generates a very high pressure in a small region above the bubble ($t = 113.84\ \mu$s). The release of the pressure wave from the impact is clearly visible from $t = 113.85\ \mu$s onwards.

formed from the rim of the bubble, but in this case the top bubble flow along the axis of symmetry is obviously faster. Therefore, the annular inflow does not reach the axis of symmetry early enough for neck closure and the normal, broad, and relatively slow jet developing from the top bubble flow by involution of the upper bubble wall takes over. The transition from the formation of a slow, broad jet to the formation of a fast, thin jet when varying D^* is very complex and proceeds with strongly distorted bubbles as shown in Fig. 5 (right diagram) for $D^* = 0.2$. Both mechanisms of jet formation are present and are of about equal importance. The struggle of vertical and horizontal flow leads to a "multiply folded" shape with tiny bubbles ejected. A complete study is very laborious and left for further work.

Perhaps the first to have seen the fast jet with bubbles collapsing very close to a solid boundary are Benjamin and Ellis [2]. They conducted experiments with expanding and collapsing bubbles at reduced ambient pressure and gave an example for $D^* \approx 0.14$. An exceedingly thin and fast jet was observed. They estimated a jet velocity of about 35 m/s at reduced ambient pressure that according

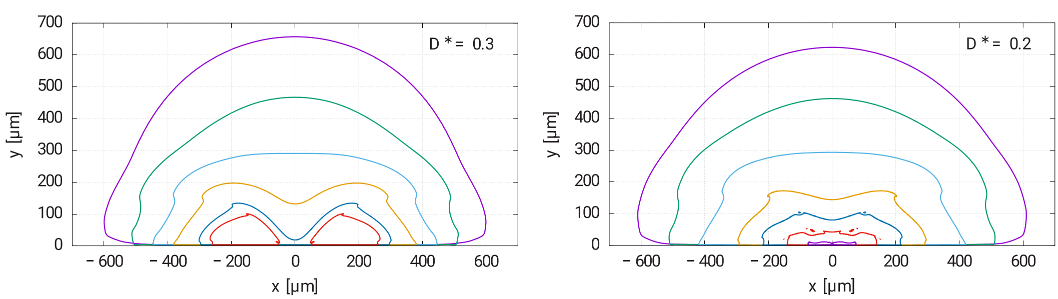

FIG. 5. Bubble shapes upon collapse. Left: $D^* = 0.3$, snapshots at $t = 55$, 90, 100, 105, 108, and 109 μs. In this case, the annular jet is too slow to reach the axis of symmetry in time before the main axial jet has passed. Right: $D^* = 0.2$, snapshots at $t = 55$, 90, 102, 108, 110, 111, and 111.3 μs. Both mechanisms of jet formation are present and are of about equal importance.

to them scales to a fivefold value (175 m/s) at atmospheric pressure. The determination of the jet velocity was limited by the time between successive frames of 0.2 ms and thus the value of 35 m/s is a lower bound, as is the 175 m/s at atmospheric pressure.

Philipp and Lauterborn [4] experimentally studied the dynamics of bubbles near a solid boundary for different D^*. They found a sharp rise in jet velocity from $D^* = 0.3$ to 0.1. Indeed, according to the present numerical study, at $D^* = 0.3$ a normal (slow) axial jet is present (Figs. 1 and 5), whereas at $D^* = 0.1$ a fast axial jet is generated by neck closure of a collapsing annular flow before the normal axial jet has time to form (not shown here). The velocity of the fast jet for $D^* = 0.1$ is approximately 1300 m/s. Philipp and Lauterborn [4] found a velocity of about 150 m/s for $D^* = 0.1$ in high-speed photographic measurements with 1-μs time intervals between successive frames. These measurements were limited by the smallness of the bubbles and the difficult optical access to the interior of the bubble to locate the jet tip. Thus, also this experimental value is a lower bound. According to the simulations, a time difference between successive frames of 10 ns would be desirable. This has been achieved with collapsing bubbles, but not for the present case [22]. Jet velocity measurements for $D^* = 0.3$ [4] gave about 40 m/s, very close to the numerical value of 38 m/s.

There have also been theoretical-numerical attempts to calculate the observed jets near solid boundaries and to determine their properties, in particular, their velocities. At first, the Rayleigh boundary case (for the nomenclature, see Ref. [14]) for spherical bubbles in an inviscid and incompressible liquid was considered [6]. For a spherical bubble touching the boundary ($D^* = 1$) a *normal, slow* axial jet with a maximum jet velocity of 130 m/s was obtained. In an extension of this work, Voinov and Voinov [7] placed an oblate spheroid slightly off the solid boundary (i.e., $D^* \gtrsim 1$) in an axisymmetric configuration. They found the phenomenon of neck closure and conjectured the possibility of fast jets by this mechanism. Jets of this type have been found experimentally [23] (see also Fig. 52 in Ref. [24], and Ref. [25]), but in a different setting of two bubbles with no direct connection to the erosion problem.

Subsequent studies on bubble collapse near solid boundaries all pertain to the normal axial jets. Thus, a breakthrough for the erosion problem can be stated by detecting these fast jets in the solution of the Navier-Stokes equations for bubbles expanding and collapsing near a solid boundary. Totally different assumptions must now be made, when considering the load of different materials by cavitation.

Both the inclusion of the expansion phase and the inclusion of viscosity in the numerical simulation are essential to get the typical bell-shaped form of the bubble during collapse and the formation of the fast axial jet observed in experiments. Neither an overexpanded exactly hemispherical bubble placed at the wall in a viscous liquid (*without* previous expansion that would lead to the characteristically deformed hemispherical bubble studied here) nor a spherical bubble with high internal pressure expanding and collapsing very close to the wall in an *inviscid* liquid show any of these phenomena. Surface tension only plays a minor role, as calculations without surface tension show. Thus the fast jets found are no capillary jets as attributed to bursting bubbles [26]. It is a topic of its own to compare the present viscosity/curvature-induced and inertia-driven jets with the large variety of jets from the bursting bubbles mentioned [26], collapsing bubbles through a hole (spherically converging induced) [27], aspherically collapsing bubbles (curvature induced) [7,28], vertically shaken liquid surfaces (surface-tension induced) [29], impinging objects (gravity induced) [30], to shaped charges (explosively driven) [31]. A complete theoretical treatment of the present fast jets is beyond the scope of this Rapid Communication. However, it is suspected that a theory will rely on subtle arguments about bubble surface curvatures and their inertia-driven evolution.

The velocity of the liquid jet for bubbles very near to the boundary could not yet reliably be measured. However, with most modern instrumentation in bubble production and high-speed photography it should be possible to visualize the extremely high-speed jets and to determine their properties. Also, many other configurations of bubbles near solid boundaries may be conceived and studied both experimentally and numerically for the appearance of fast jets. These fast and thin jets can generate impact pressures on the solid surface well in the GPa range. Thus they are prime candidates for bubble erosion, in particular, of hard, solid surfaces.

The authors thank the Cavitation Bubble Dynamics Group at the Drittes Physikalisches Institut for many inspiring discussions. The work was supported in part by the Deutsche Forschungsgemeinschaft (German Science Foundation) under Contract Me 1645/8-1. C.L. thanks H. C. Kuhlmann and the Institute of Fluid Mechanics and Heat Transfer, TU Wien, for their hospitality. Computational resources on the cae cluster of TU.it, TU Wien, are gratefully acknowledged.

---

[1] C. F. Naudé and A. T. Ellis, On the mechanism of cavitation damage by nonhemispherical cavities collapsing in contact with a solid boundary, J. Basic Eng. **83**, 648 (1961).

[2] T. B. Benjamin and A. T. Ellis, The collapse of cavitation bubbles and the pressures thereby produced against solid boundaries, Philos. Trans. R. Soc., A **260**, 221 (1966).

[3] Y. Tomita and A. Shima, Mechanisms of impulsive pressure generation and damage pit formation by bubble collapse, J. Fluid Mech. **169**, 535 (1986).

[4] A. Philipp and W. Lauterborn, Cavitation erosion by single laser-produced bubbles, J. Fluid Mech. **361**, 75 (1998).

[5] J. R. Krieger and G. L. Chahine, Acoustic signals of underwater explosions near surfaces, J. Acoust. Soc. Am. **118**, 2961 (2005).

[6] M. S. Plesset and R. B. Chapman, Collapse of an initially spherical vapour cavity in the neighbourhood of a solid boundary, J. Fluid Mech. **47**, 283 (1971).

[7] O. V. Voinov and V. V. Voinov, On the process of collapse of a cavitation bubble near a wall and the formation of a cumulative jet, Sov. Phys. Doklady. **21**, 133 (1976).

[8] A. Shima and Y. Sato, The collapse of a bubble attached to a solid wall, Ing. Arch. **48**, 85 (1979).

[9] J. R. Blake, Y. Tomita, and R. P. Tong, The art, craft and science of modelling jet impact in a collapsing cavitation bubble, Appl. Sci. Res. **58**, 77 (1998).

[10] C.-T. Hsiao, A. Jayaprakash, A. Kapahi, J.-K. Choi, and G. L. Chahine, Modelling of material pitting from cavitation bubble collapse, J. Fluid Mech. **755**, 142 (2014).

[11] Q. Wang, W. Liu, A. M. Zhang, and Y. Sui, Bubble dynamics in a compressible liquid in contact with a rigid boundary, Interface Focus **5**, 20150048 (2015).

[12] M. Koch, C. Lechner, F. Reuter, K. Köhler, R. Mettin, and W. Lauterborn, Numerical modeling of laser generated cavitation bubbles with the finite volume and volume of fluid method, using OpenFOAM, Comput. Fluids **126**, 71 (2016).

[13] C. Lechner, M. Koch, W. Lauterborn, and R. Mettin, Pressure and tension waves from bubble collapse near a solid boundary: A numerical approach, J. Acoust. Soc. Am. **142**, 3649 (2017).

[14] W. Lauterborn, C. Lechner, M. Koch, and R. Mettin, Bubble models and real bubbles: Rayleigh and energy-deposit cases in a Tait-compressible liquid, IMA J. Appl. Math. **83**, 556 (2018).

[15] Typical yield stresses of hard metals and ceramics fall in the range of about 200–1000 MPa, while the jet impact pressure at 100 m/s can be approximated by the water hammer pressure as 150 MPa.

[16] I. Akhatov, O. Lindau, A. Topolnikov, R. Mettin, N. Vakhitova, and W. Lauterborn, Collapse and rebound of laser-induced cavitation bubbles, Phys. Fluids **13**, 2805 (2001).

[17] S. Fujikawa and T. Akamatsu, Effects of the non-equilibrium condensation of vapour on the pressure wave produced by the collapse of a bubble in a liquid, J. Fluid Mech. **97**, 481 (1980).

[18] The OpenFOAM(R) Extend Project. http://sourceforge.net/projects/openfoam-extend/.

[19] C. W. Hirt and B. D. Nichols, Volume of fluid (VOF) method for the dynamics of free boundaries, J. Comput. Phys. **39**, 201 (1981).

[20] See Supplemental Material at http://link.aps.org/supplemental/10.1103/PhysRevFluids.4.021601 for a brief description of the numerical model and setup as well as three-dimensional views of the bubble shapes.

[21] In contrast, in the inviscid theory, a (nearly perfect) hemispherical cavity would be obtained with a completely different dynamics, i.e., an essentially spherical collapse.
[22] O. Lindau and W. Lauterborn, Cinematographic observation of the collapse and rebound of a laser-produced cavitation bubble near a wall, J. Fluid Mech. **479**, 327 (2003).
[23] W. Lauterborn, Optische Kavitation (Optic cavitation), Phys. Bl. **32**, 553 (1976).
[24] W. Lauterborn, T. Kurz, R. Mettin, and C. D. Ohl, Experimental and theoretical bubble dynamics, Adv. Chem. Phys. **110**, 295 (1999).
[25] B. Han, K. Köhler, K. Jungnickel, R. Mettin, W. Lauterborn, and A. Vogel, Dynamics of laser-induced bubble pairs, J. Fluid Mech. **771**, 706 (2015).
[26] L. Deike, E. Ghabache, G. Liger-Belair, A. K. Das, S. Zaleski, S. Popinet, and T. Séon, Dynamics of jets produced by bursting bubbles, Phys. Rev. Fluids **3**, 013603 (2018).
[27] S. R. Gonzalez Avila, C. Song, and C.-D. Ohl, Fast transient microjets induced by hemispherical cavitation bubbles, J. Fluid Mech. **767**, 31 (2015).
[28] W. Lauterborn, Cavitation bubble dynamics - new tools for an intricate problem, Appl. Sci. Res. **38**, 165 (1982).
[29] B. W. Zeff, B. Kleber, J. Fineberg, and D. P. Lathrop, Singularity dynamics in curvature collapse and jet eruption on a fluid surface, Nature (London) **403**, 401 (2000).
[30] S. Gekle, J. M. Gordillo, D. van der Meer, and D. Lohse, High-Speed Jet Formation After Solid Object Impact, Phys. Rev. Lett. **102**, 034502 (2009).
[31] G. Birkhoff, D. P. MacDougall, E. M. Pugh, and S. G. Taylor, Explosives with lined cavities, J. Appl. Phys. **19**, 563 (1948).